RESEARCH ARTICLE | NOVEMBER 26 2013

Low-energy positron scattering from gas-phase tetrahydrofuran: A quantum treatment of the dynamics and a comparison with experiments

J. Franz; F. A. Gianturco

J. Chem. Phys. 139, 204309 (2013)
https://doi.org/10.1063/1.4832417

Low-energy positron scattering from gas-phase tetrahydrofuran: A quantum treatment of the dynamics and a comparison with experiments

J. Franz[1,a] and F. A. Gianturco[2]
[1]*Mulliken Center for Theoretical Chemistry, University of Bonn, Beringstr. 4-6, 53115 Bonn, Germany*
[2]*Department of Chemistry, The University of Rome Sapienza, Piazzale A. Moro 5, 00185 Rome, Italy*

(Received 19 June 2013; accepted 7 November 2013; published online 26 November 2013)

In this paper we report new quantum calculations of the dynamics for low-energy positrons interacting with gaseous molecules of tetrahydrofuran. The new quantum scattering cross sections are differential and integral cross sections at collision energies between 1.0 and 25.0 eV and include a careful treatment of the additional effects on the scattering process brought about by the permanent dipole moment of the target molecule. The present results are compared with an extensive range of measured data, both for the angular distributions and for the elastic integral cross sections and agree remarkably well with all findings. The new calculated quantities reported here also show the importance of correcting the experimental integral cross sections for the angular discrimination in the forward direction. © *2013 AIP Publishing LLC*. [http://dx.doi.org/10.1063/1.4832417]

I. INTRODUCTION

More than ten years ago the seminal experiments of Leon Sanche's group in Sherbrooke[1] have shown very convincingly that sub-excitation electrons interacting with DNA materials can cause the presence of specific resonant processes which would eventually lead to single- or double strand break (SSB or DSB) effects and therefore, to the permanent damaging of the biological structures and roles of that important molecule in the cell.

Since then a great deal of work has been carried out to find additional evidence and additional molecular examples among the DNA components that would confirm and extend the findings of that initial work (for more recent discussions and references see Refs. 2–4) and therefore the area of following, either via experiments or by computational models, the path to electron interactions with biomolecular systems has grown into a well established realm of study.

In analogy with the above growth, the use of low-energy positron beams on biosystems has also become a clearly more active area of study, so that the consequences of using the electron's antiparticle in gas-phase molecular systems have been analysed and discussed in several recent papers since positrons can also potentially induce damage of the biological environments via direct ionization by the thermalising positron beam, via the release of a substantial swarm of secondary electrons, or by opening new channels like positrononium (Ps) formation and gamma-ray emission upon annihilation, all events which can trigger additional damage with respect to that from an electrons' beam (see, e.g., Ref. 5).

The number of experimental studies which directly deal with positron beams, however, has been much smaller than in the case of electrons and therefore, it becomes increasingly more necessary to provide for the few cases that exist, or that are being discussed in the literature, a reliable set of either experimental observations or of computational benchmarks which could confirm (or contradict) what has been observed on a specific system.

The recent experimental data on a molecular derivative with great relevance in the biological analysis of collision-induced damaging effects has been the tetrahydrofuran (THF) molecular system,[9] a molecular component that has received attention also for electron scattering processes.[6–9] In particular, Fuss *et al.*[9] provide an extensive and thorough analysis of all of the existing data on the THF molecule.

In the present work, therefore, we have realized that to have novel computational assessments of the integral (ICS) and differential (DCS) cross sections for low-energy positron scattering off gas-phase THF, can indeed provide an additional set of data on the behaviour of this molecule in its interactions with the electron's antiparticle and for the same channels which have recently been measured on this system.[26] In our computations we do not take into account inelastic channels like Positronium formation, annihilation, ionization, and vibrational or electronic excitation, because such a treatment is computationally too demanding. Annihilation is possible at all collision energies, but the coupling to the elastic channels is usually small.[10] The couplings between open channels usually will give structure in the elastic cross section on either side of each threshold for opening a new inelastic channel, and a detailed discussion of this feature can be found in Charlton and Humberston.[10] The effects on the structure of the elastic cross section is expected to be much smaller than the uncertainties in positron beam experiments with molecular targets. Therefore, it should be a valid assumption to neglect these channels in the comparison of elastic cross sections. The threshold for Positronium formation is given by $E_{Ps} = E_{ion} - 6.8\,eV$.[10] The experimental value for the first ionization energy (at the peak maximum)

[a]Present address: Department of Atomic, Molecular and Optical Physics, Faculty of Applied Physics and Mathematics, Gdansk University of Technology, ul. Narutowicza 11/12, PL 80-233 Gdansk, Poland; Electronic mail: j.franz@ucl.ac.uk

was measured by Potts *et al.*[11] to be $E_{\rm ion} \approx 9.4$ eV, which gives $E_{\rm Ps} \approx 2.8$ eV.

Section II reports our computational method while Sec. III provides our results and compares them with the existing data, both experimentally and computationally, acquired for positron scattering.

Our final comments on our findings and our present conclusions are collected in Sec. IV.

II. THEORETICAL AND COMPUTATIONAL METHODS

A. Scattering equations

In order to obtain the scattering cross sections for polyatomic molecules, we need to solve the Schrödinger equation of the total system

$$(H - E)\Psi = 0 \tag{1}$$

at the total energy E, for the corresponding wavefunction Ψ. Here H is the total Hamiltonian given by

$$H = H_{mol} + K + V, \tag{2}$$

where H_{mol}, K, and V represent the operators of the molecular Hamiltonian, kinetic energy for the scattered positron, and the interaction potential between the incident positron and the target molecule, respectively. The H_{mol} further consists, in general, of the rotational and vibrational parts

$$H_{mol} = H_{rot} + H_{vib}, \tag{3}$$

whereby we exclude, at the collision energies considered, electronic excitations, ionization, and the Ps formation channels.

The total wavefunction Ψ is described in the body-fixed (BF) reference frame, in which the z axis is taken along the direction of the main molecular axis and is expanded around a single-centre (SCE) as

$$\Psi(\mathbf{r}_1 ... \mathbf{r}_Z, \mathbf{r}_p|\mathbf{R}) = \Psi_{mol}(\mathbf{r}_1 ... \mathbf{r}_Z|\mathbf{R})\varphi(\mathbf{r}_p|\mathbf{R}), \tag{4}$$

where

$$\varphi(\mathbf{r_p}|\mathbf{R}) = \sum_{l\pi\mu h} r_p^{-1} u_{lh}^{\pi\mu}(r_p|\mathbf{R}) X_{hl}^{\pi\mu}(\hat{\mathbf{r}}_p). \tag{5}$$

In Eq. (4), $\mathbf{r_i}$ represents the position vector of the ith electron among the Z bound electrons in the target, taken from the centre of mass. Ψ_{mol} is the electronic wavefunction for the molecular target at the nuclear geometry $\mathbf{R}$. The continuum function $\varphi(\mathbf{r_p}|\mathbf{R})$ refers to the wavefunction of the scattered positron under the full action of the field created by the molecular electrons and by their response to the impinging positron as described in Ref. 13. Each $u_{lh}^{\pi\mu}$ is the radial part of the wavefunction for the incident particle and the $X_{hl}^{\pi\mu}$ are the symmetry-adapted angular basis functions (for more detailed information see, e.g., Ref. 12). The suffix π stands for the irreducible representation (IR), μ distinguishes the components of the basis, if its dimension is greater than one, and h does the same within the same set with angular momentum quantum number l.

We can now assume that the target molecule can be kept fixed during the collision, since the molecular rotations and vibrations are often slower when compared with the velocity of the impinging positrons considered in the present study. This is called the fixed-nuclear (FN) approximation[14] that ignores the molecular term of H_{mol} in Eq. (2) and fixes the values of all $\mathbf{R}$ at their equilibrium locations in the target molecule. To solve the Schrödinger equation in the FN approximation, we make use of the body-fixed (BF) system rather than the laboratory frame, space-fixed (SF) frame of reference, because a formulation in the former can be simpler, both conceptually and computationally. The two systems are related through a frame transformation scheme given, for example, by Chang and Fano.[14]

After substituting Eq. (4) into (1) under the FN approximation, we obtain a set of coupled differential equations for u_{lv}, where, for simplicity, v represents $(\pi\mu h)$ collectively:

$$\left\{\frac{d^2}{dr_p^2} - \frac{l(l+1)}{r_p^2} + k^2\right\} u_{lv}(r_p|\mathbf{R}) = 2\sum_{l'v'} \langle lv|\mathbf{V}|l'v'\rangle u_{l'v'}(r_p|\mathbf{R}) \tag{6}$$

with

$$\langle lv|\mathbf{V}|l'v'\rangle = \int d\hat{r}_p X_{lv}^*(\hat{r}_p) V(r_p|\mathbf{R}) X_{l'v'}(\hat{r}_p). \tag{7}$$

When solving Eq. (6) under the boundary conditions that the asymptotic form of u_{lv} is represented by a sum consisting of outgoing spherical Bessel- and Neumann functions, we obtain the corresponding S-matrix elements, $S_{l'v'}^{lv}$. The actual numerical procedure we have employed to solve that equation is given in detail in Refs. 15 and 16.

The integral cross section (ICS) for the elastic scattering in the BF frame is given by

$$\sigma_{cc} = \frac{\pi}{k^2} \sum_{lv} \sum_{l'v'} |T_{l'v'}^{lv}|^2, \tag{8}$$

where the index cc indicates the close-coupling approach.

The **T**-matrix is defined as a function of the **S** and **K**-matrices:

$$\mathbf{T} = 1 - \mathbf{S} \tag{9}$$

$$= 1 - (1 - i\mathbf{K}) \cdot (1 + i\mathbf{K})^{-1}\,. \tag{10}$$

The integral cross section diverges in the forward scattering direction in the presence of a molecular dipole moment, because of the long-range interaction between the positron and the molecular dipole moment. This problem can be solved by applying the following closure formula for the differential cross section:[24]

$$\frac{d\sigma}{d\Omega}(J\tau \to J'\tau') = \frac{d\sigma_{\rm rd}^B}{d\Omega}(J\tau \to J'\tau') + \sum_L (A_L - A_L^B) P_L(\cos\theta), \tag{11}$$

where $J\tau$ and $J\prime\tau\prime$ denote the initial and final rotational levels, respectively. The first quantity on the right-hand side is the differential cross section for a rotating dipole using the first Born approximation. The $P_L(\cos\theta)$ are the Legendre functions. The coefficients A_L are computed from the **K**-matrices, which are obtained by solving the close-coupling equations. The coefficients A_L^B are computed from the **K**-matrices using

the first Born approximation. Explicit formulas for A_L and A_L^B are given in Gianturco and Jain.[12] The final differential cross section is obtained by summation over the different initial and final rotational levels:

$$\frac{d\sigma}{d\Omega} = \sum_{J\tau J'\tau'} \frac{d\sigma}{d\Omega}(J\tau \rightarrow J'\tau'). \tag{12}$$

The corresponding integral cross section in the SF frame can be computed as

$$\sigma = \sigma_{rd}^B + \sigma_{cc} - \sigma_{fd}^B. \tag{13}$$

Here σ_{rd}^B is the integral cross section for a rotating dipole in the Born approximation. σ_{cc} is the integral cross section obtained by solving the close-coupling equations in the FN-approximation and σ_{fd}^B is the integral cross section for a fixed dipole. Further details can be found in Sanna and Gianturco.[24]

B. The density functional theory (DFT) modelling of correlation and polarization

The interaction between the positron and the molecular nuclei and electrons is specified by the total interaction potential

$$V_{\rm tot}(\mathbf{r}_e|\mathbf{R}) = V_{\rm st}(\mathbf{r}_e|\mathbf{R}) + V_{\rm pcp}(\mathbf{r}_e|\mathbf{R}), \tag{14}$$

which is the sum of the static potential $V_{\rm st}$ and the correlation-polarization potential $V_{\rm pcp}$. The static potential $V_{\rm st}$ is the exact electro-static interaction potential between the positron and the nuclei and electrons in the molecule. The correlation-polarization potential is modeled by the potential[16]

$$V_{\rm pcp}(\mathbf{r}_e|\mathbf{R}) = \begin{cases} V_{\rm corr}(\mathbf{r}_e|\mathbf{R}) \text{ for } r_p \le r_c \\ V_{\rm pol}(\mathbf{r}_e|\mathbf{R}) \text{ for } r_p > r_c \end{cases}. \tag{15}$$

Here $V_{\rm corr}$ and $V_{\rm pol}$ are the short-range and long-range parts of the correlation-polarization potential, respectively. r_c is the outermost point, at which $V_{\rm pol}$ becomes larger than $V_{\rm corr}$. $V_{\rm corr}$ is based on the functional $\epsilon^{\rm e-p}[\rho(\mathbf{r}_e|\mathbf{R})]$ for the correlation energy of one positron in an electron gas with density $\rho(\mathbf{r}_e|\mathbf{R})$. Boronski and Nieminen[17] have derived interpolation formulae for $\epsilon^{\rm e\text{-}p}$. $V_{\rm corr}$ can be obtained from $\epsilon^{\rm e\text{-}p}$ by the functional derivative[16]

$$V_{\rm corr}(\mathbf{r}_e|\mathbf{R}) = \frac{\delta}{\delta\rho}\left\{\epsilon^{\rm e-p}[\rho(\mathbf{r}_e|\mathbf{R})]\right\}. \tag{16}$$

The long-range part $V_{\rm pol}$ of the correlation-polarization potential is given by

$$V_{\rm pol}(\mathbf{r}_e|\mathbf{R}) = -\left(\frac{\alpha_0}{2r^4} + \frac{\alpha_2}{2r^4}P_2(\cos\theta)\right), \tag{17}$$

where α_0 and α_2 are the values of the isotropic and anisotropic polarizabilities, respectively, and $P_2(cos\theta)$ is a Legendre polynomial.

C. Computational details

The target molecule is constrained to its equilibrium structure that belongs to the C_{2v} symmetry. The molecular geometry and the ground state molecular orbitals are generated with the Gaussian 09 program package employing the Perdew-Burke-Ernzerhof (PBE) density functional and aug-cc-pVTZ basis set.[18] The computed molecular dipole moment is 1.75 D, which is a small overestimation of the the experimental value of 1.63 D by Gent.[19] Our computed rotational constants are $A = 6.95$ GHz, $B = 6.86$ GHz, and $C = 3.78$ GHz. This is in good agreement with the values by Melnik *et al.*:[20] 7.10, 6.98, and 4.01 GHz, obtained by fitting microwave spectra to a parameterized Hamiltonian. However, Melnik *et al.* are using a slightly different definition of these parameters in their Hamiltonian, which gives limits to the assessment of this comparison. With the PBE-functional, the elements of the polarizability tensor are computed to be $\alpha_{xx} = 48.0$ bohr^3, $\alpha_{yy} = 67.8$ bohr^3, and $\alpha_{zz} = 55.1$ bohr^3. Jansik *et al.*[21] have shown that polarizabilities computed with DFT are in good agreement with *ab initio* coupled cluster response theory.

The single-centre-expansions of the molecular electron density and of the potential are done with an improved version of the SCELib3.0 computational library,[22] to which we have added the correlation-polarization potential specific for modeling the interactions of the molecular electrons with slow positrons. The coupled scattering equations are solved by Volterra integration, using an improved version of the VOLSCAT program package.[23] The grid for the radial integration ranges up to 521 bohrs. More specifically the VOLSCAT suite of codes computes the integral cross section in the BF-frame (denoted previously as σ_{cc}) and therefore generates the necessary body-fixed **K**-matrices.

The body-fixed **K**-matrices are then processed by the program package POLYDCS,[24] that transforms the body-fixed **K**-matrices into the space-fixed **K**-matrices and further applies the Born correction, as outlined by Sanna and Gianturco.[24] From the space-fixed **K**-matrices obtained in this way we can further generate the state-to-state rotationally elastic and inelastic differential and integral cross sections. During the frame transformation step of the present calculations the rotational eigenfunctions and eigenvalues for the asymmetric top are in turn generated using the program ASYMTOP of Jain and Thompson[25] with our computed rotational constants.

III. RESULTS AND DISCUSSION

A. Differential cross sections

The various differential cross sections for a collision energy of 1.0 eV are shown in Figure 1. All DCSs are folded at 90°. The *ab initio* results are shown by the solid black line. The experimental values of Chiari *et al.*[26] are also shown together with their theoretical values, which were obtained by using the IAM-SCAR (independent atom model with screening corrected additivity rule) method, a model pseudopotential method employed successfully at higher collision energies, as discussed in previous work,[27,28] but which has usually been less accurate than the *ab initio* methods when discussing electron-molecule scattering at the lower collision energies as those shown here for positron collisions.[27,28] In order to get some data on the importance of the molecular dipole moment on the size of the elastic cross section, we also

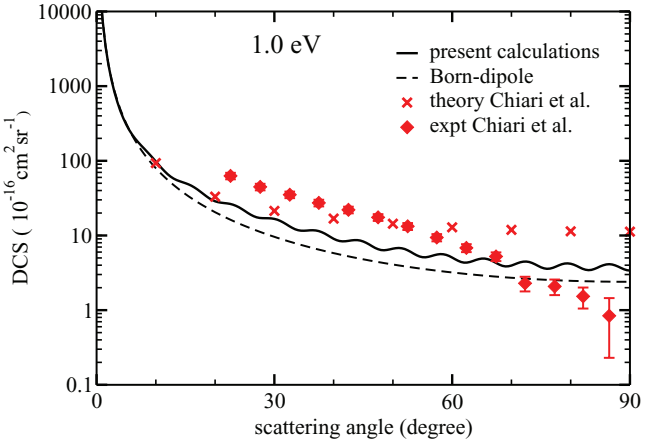

FIG. 1. Computed and measured differential cross sections for positron scattering off gas-phase THF at a collision energy of 1.0 eV. Shown are our corrected close coupling results (solid black line) using $l_{max} = 50$ and summing over rotational elastic and inelastic channels, the Born-dipole results (dashed black line) and the data by Chiari *et al.*:[26] experimental (red diamonds with error bars) and theoretical (red crosses).

show the differential cross section using just the first Born approximation for the dipole potential, which is given by[12]

$$\frac{d\sigma_{rd}^{B}}{d\Omega}(0_0 \rightarrow 1_0) = \frac{4D^2}{3}\frac{k'}{k}\frac{1}{(k^2 + k'^2 - 2kk'\cos\theta)}, \qquad (18)$$

and is shown by the dashed black line in the figure. Here D is the molecular dipole moment, $k = \sqrt{2E}$, $k' = \sqrt{2(E - \epsilon_{rot}(0_0 \rightarrow 1_0))}$, E is the collision energy, and $\epsilon_{rot}(0_0 \rightarrow 1_0)$ is the energy difference between the rotational levels $J'_{\tau'} = 1_0$ and $J_\tau = 0_0$.

We see that at low energies the present results follow the general trend of marked increase in the forward direction, while agreeing more closely with the model calculations of Chiari *et al.*[26] However, for angles beyond 40°, where the DCS values become much smaller, the present calculations again follow the experimental trend, as well as the Born-dipole cross sections.

The comparison between measured and calculated DCS at 2.0 eV of collision energy, shown in Figure 2, largely follows the previous trend, with the agreement with the experiments setting in at even smaller angles (i.e., for $\theta \leq 60°$). The agreement between the present calculations and the measured

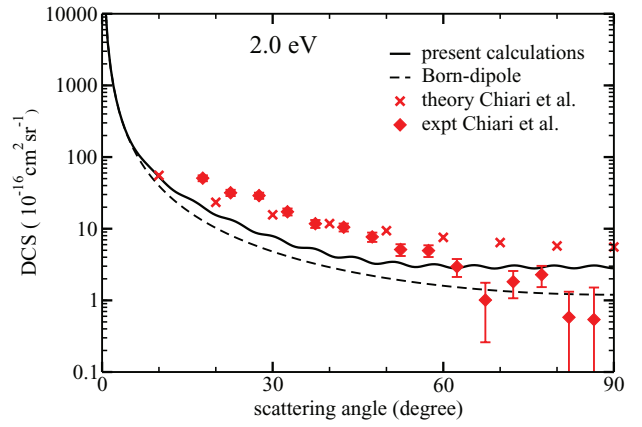

FIG. 2. Same as Figure 1 for a collision energy of 2.0 eV.

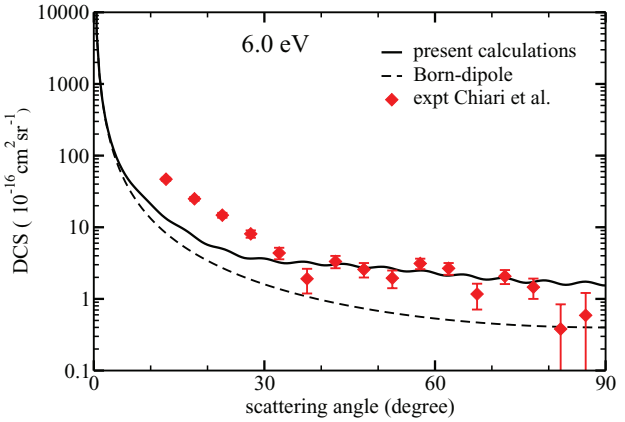

FIG. 3. Same as Figure 1 for a collision energy of 6.0 eV.

data of Chiari *et al.*[26] as the collision energy increases is confirmed by the data reported in Figure 3 at 6.0 eV of collision energy. We see there, in fact, that our calculations, beside increasing in the forward direction like the experiments, quantitatively agree with the measured data from 30° onwards.

Figures 4–7 report in detail the behaviour of the DCS at four different collision energies: at 8.0, 10.0, 20.0, and 25.0 eV. All the data in all the panels continue to show the same trend as that of the lower energies: the quantitative agreement between the present calculations and the experimental DCS extends over a larger angular range as the collision energy increases. At 20.0 and 25.0 eV, therefore we see that the data essentially coincide with the experiments from about 20° onwards. At 10.0 and 20.0 eV, computations are also close to the model calculations reported on THF in Ref. 26.

We can therefore conclude from this analysis of the DCS behaviour that the present calculations provide thus far the best available agreement between calculated and measured DCS values over a fairly broad range of collision energies, therefore lending additional confidence to our knowledge of the size and shape of the scattered positrons from gaseous THF.

B. Integral cross sections

Figure 8 shows the computed integral cross sections for various partial wave expansions. The thick lines in the lower

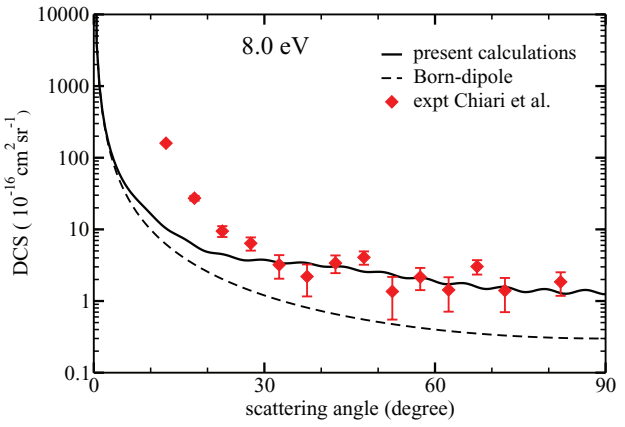

FIG. 4. Same as Figure 1 for a collision energy of 8.0 eV.

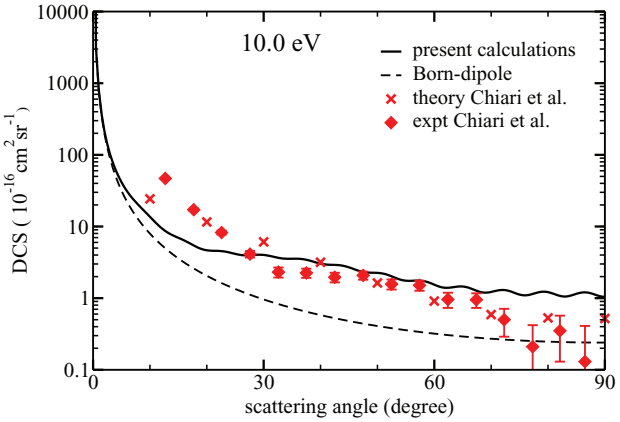

FIG. 5. Same as Figure 1 for a collision energy of 10.0 eV.

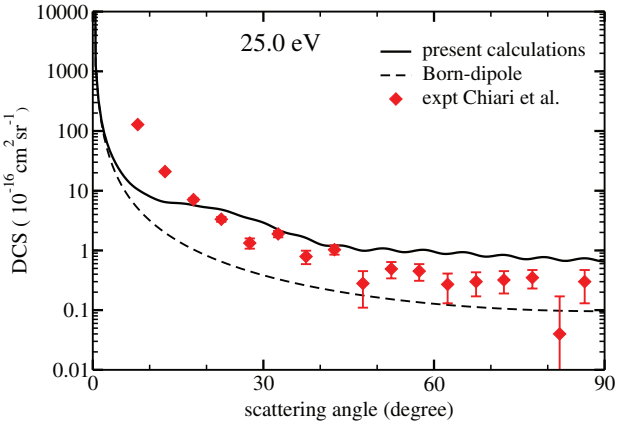

FIG. 7. Same as Figure 1 for a collision energy of 25.0 eV.

part of the panel show the cross sections computed in the BF frame, while the thin lines show the integral cross sections after applying the Born dipole correction in the SF reference frame and summing over the rotational elastic and inelastic channels as carried out in our POLYDCS-code.[24] In the summation over rotational channels the zeroth level is included as initial state and the first five states as final rotational channels. One can see that the convergence of the results in the body frame is slow with respect to the partial wave expansion. In the SF calculation all the computed cross sections are instead very close to each other and the convergence with respect to the partial wave expansion is very fast. In fact, the results for $l_{max} = 20$ do not differ very much from the results for $l_{max} = 50$.

Figure 9 further compares our results with the experimental and computational data of Chiari *et al.*[26] and with the experimental data of Zecca *et al.*[6] Our computations use the partial wave expansion up to $l_{max} = 50$ after including the Born dipole correction in the SF frame and summing over rotational elastic and inelastic channels. They are shown by the solid black line in the figure.

In both experiments the linear transmission technique is used. This means that, within a specific angular cone in the forward direction, it is not possible to distinguish between particles that are scattered elastically in the forward direction and unscattered particles (see, e.g., Sullivan *et al.*[29] for a general discussion). In the experimental setups in Trento and at Australian National University (ANU) a retarding potential technique is employed to analyse the scattered positrons. For this kind of setup Kauppila *et al.*[30] and Kwan *et al.*[31] have derived an expression for estimating the angle θ_{min}, which describes the forward angular cone as a function of the retarding potential ΔV and the collision energy E by the relation

$$\theta_{min} = \sin^{-1}\sqrt{\frac{e\Delta V}{E}}, \tag{19}$$

where e is the elementary charge. In order to correct the experimental data for the particles scattered into the forward cone, we have added to the experimental data the following part,

$$\Delta\sigma_E^{forward} = 2\pi \cdot \int_0^{\theta_{min}} \frac{d\sigma_{calc}}{d\Omega} \sin\theta d\theta, \tag{20}$$

which contains the integral over our computed differential cross sections $\frac{d\sigma_{calc}}{d\Omega}$ carried out between the forward direction and the angular discrimination angle θ_{min}.

The experimental data by Chiari *et al.*[26] are shown by the full red diamonds. For this comparison we have used the

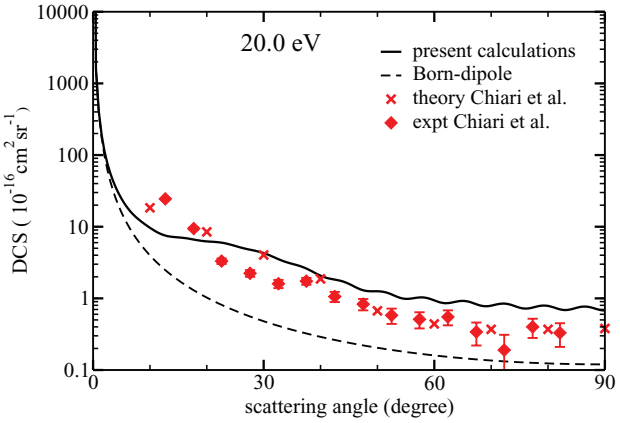

FIG. 6. Same as Figure 1 for a collision energy of 20.0 eV.

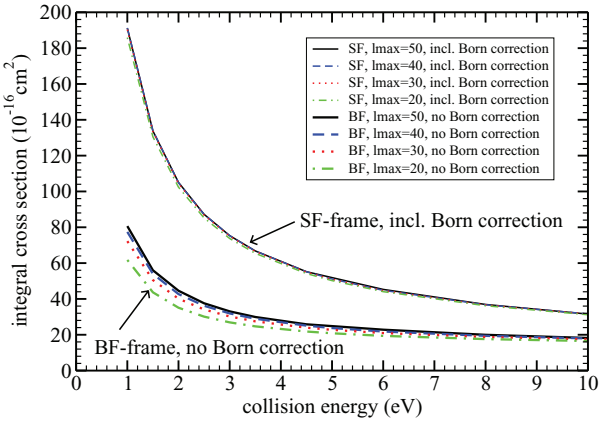

FIG. 8. Computed integral cross sections for positron scattering off gas-phase THF using different partial wave expansions. The thick lines represent computations in the body-fixed (BF) frame. The thin lines are the calculations done in the space-fixed (SF) frame including Born dipole correction and summation over rotational elastic and inelastic channels.

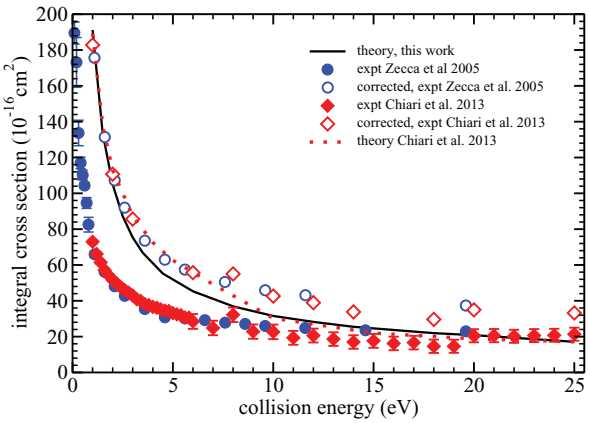

FIG. 9. Computed and measured integral cross sections for positron scattering off gas-phase THF. The computed results from this paper are shown by the solid black line. In this computation a partial wave expansion up to $l_{max} = 50$ is used. The results include the Born dipole correction in the space-fixed (SF) frame and the summation over rotational elastic and inelastic channels. The experimental data by Chiari *et al.*[26] are shown by the full red diamonds with error bars and by open red diamonds after correction for forward scattering. The experimental data by Zecca *et al.*[6] are shown by full blue circles with error bars and by open blue circles after correction for forward scattered positrons. The dotted red line shows the computations by Chiari *et al.*[26] using the IAM-SCAR method. See text for further details.

elastic cross section

$$\sigma_E = \sigma_T - \sigma_{Ps} - \sigma_I \ , \tag{21}$$

which we obtained by subtracting the measured cross sections for Positronium formation σ_{Ps} and Ionization σ_I from the measured total cross section σ_T. The error bars shown are errors ($\Delta\sigma_T$) given in Ref. 26 for the total cross section. They used a retarding potential $\Delta V = 120$ mV, which is an offset of 3-4 standard deviations of the beam energy distribution. The experimental values of Chiari *et al.*, corrected by this procedure, are given by the open red diamonds in the figure. We have corrected most of the experimental values with computational cross sections at the same energy. However, at collision energies of 1.6 eV, 2.6 eV, 3.6 eV, and 4.6 eV the corrections are made with computations done at energies which are 0.1 eV lower.

The experimental data by Zecca *et al.*[6] are shown by full blue circles. After applying the correction as outlined above and using a value of $\Delta V = 90$ mV for the retarding potential used in the Trento experiments, we obtain the data points shown by open blue circles. Most of the corrections are done at similar energies, however, the experimental values at collision energies of 1.1 eV, 1.6 eV, 2.1 eV, 2.6 eV, 3.6 eV, and 4.6 eV are corrected by calculations done at collision energies, which are 0.1 eV lower, and the experimental values at 5.6 eV, 7.6 eV, 9.6 eV, 11.6 eV, and 19.6 eV are corrected by computations for collisions, which are 0.4 eV higher in energy.

The computations by Chiari *et al.*[26] using the IAM-SCAR method discussed before[27,28] are shown by the dotted red line. For these numbers we included the elastic and rotational inelastic cross sections

$$\sigma_{E+rot}^{IAM-SCAR} = \sigma_{E}^{IAM-SCAR} + \sigma_{rot}^{IAM-SCAR}, \tag{22}$$

as given in Table 3 of Chiari *et al.*[26] One clearly sees from the extensive comparison of Figure 9 that the present calculations, which do not contain empirical parameters in the potential for the scattering process, are producing very good agreement with existing experiments.

IV. PRESENT CONCLUSIONS

The work discussed in the previous section addresses the problem of producing from quantum scattering calculations the low-energy scattering behaviour of a beam of positrons and gaseous THF molecules.

The existence of two sets of experiments,[6,26] which agree very well with each other in the size and shape of their ICS, and which suffer both from similar angular discrimination errors, enticed us to see whether or not an *ab initio* approach could be successfully employed to correct for the effects of positrons scattered in the forward direction and to obtain agreement between experiment and theory.

We have therefore employed our multichannel scattering code that describes polarization and correlation effects induced by the impinging positron projectile and that analyses the scattering event via a partial wave expansion of the continuum projectile. The details of our method are outlined in Sec. II and the special features imposed by the presence of a permanent dipole moment in THF are also discussed there in terms of corrections to the BF results for the cross sections.

The calculations of the scattered angular distribution (DCS) are reported in Sec. III, where they are also compared with available experimental data: the agreement is very good once outside the forward scattering cone and it gets increasingly better as the energy is increased. The angular distributions provided at a few energies by the model potential IAM-SCAR method also turn out to be in good accord with our *ab initio* data.

The additional comparison between the existing experiments from two different groups[6,26] and our calculated ICS, shown in detail in Figure 9 over a broad range of collision energies, indicates a good accord between our calculations and both experiments, thereby confirming both sets of data.

We can therefore say that the integral and differential elastic cross sections for low-energy positron scattering by THF molecules are now confirmed in size and shape both by two experiments and by the present theoretical calculations.

ACKNOWLEDGMENTS

This work was carried out under the HPC-EUROPA2 project (Project No. 228398) with the support of the European Commission Capacities Area – Research Infrastructures Initiative. This work has been supported by the COST Action MP 1002 – Nano-scale Insights into Ion Beam Cancer Therapy. The financial support of CASPUR and CINECA computational grants is gratefully acknowledged. J.F. thanks the staff at CINECA for their kind hospitality and support. We thank Isabella Baccarelli, Sergio Orlandini, Mario Tacconi, and Nico Sanna of CINECA for maintaining the SCELib software package. We thank Luca Chiari (Flinders University and ANU Canberra) for telling us about

the angular discrimination function of the machine in Trento, which was used in the experiments by Zecca *et al.*[6]

[1]B. Boudaiffa, P. Clouthier, D. Hunting, M. A. Huels, and L. Sanche, Science **287**, 1658 (2000).
[2]I. Baccarelli, I. Bald, F. A. Gianturco, E. Illenberger, and J. Kopyra, Phys. Rep. **508**, 1 (2011).
[3]B. A. Huber, C. Malot, A. Domaracka, and A. Solovjov, J. Phys.: Conf. Ser. **373**, 011001 (2012).
[4]*Radiation Damage in Biomolecular Systems*, edited by G. Garcia Gómez-Tejedor and M. C. Fuss (Springer, Berlin, 2012).
[5]M. J. Brunger, S. J. Buckman, and A. Zecca, J. Phys.: Conf. Ser. **194**, 012034 (2009).
[6]A. Zecca, C. Perazzolli, and M. J. Brunger, J. Phys. B **38**, 2079 (2005).
[7]P. Mozejko, E. Ptasinska-Denga, A. Domaracka, and C. Szmytkowski, Phys. Rev. A **74**, 012708 (2006).
[8]M. Allan, J. Phys. B **40**, 3531 (2007).
[9]M. Fuss, A. Munoz, J. C. Oller, F. Blanco, D. Almeida, P. Limao-Vieira, T. P. T. Do, M. J. Brunger, and G. Garcia, Phys. Rev. A **80**, 052709 (2009).
[10]M. Charlton and J. W. Humberston, *Positron Physics* (Cambridge University Press, Cambridge, 2001).
[11]A. Giuliani, P. Limao-Vieira, D. Duflot, A. R. Milosavljevic, B. P. Marinkovic, S. V. Hoffmann, J. Delwiche, and M.-J. Hubin-Franskin, Eur. Phys. J. D **51**, 97 (2009).
[12]F. A. Gianturco and A. Jain, Phys. Rep. **143**, 347 (1986).
[13]J. Franz, F. A. Gianturco, K. L. Baluja, J. Tennyson, R. Carey, R. Montuoro, R. R. Lucchese, T. Stoecklin, P. Nicholas, and T. L. Gibson, Nucl. Instrum. Methods Phys. Res. B **266**, 425 (2008).
[14]E. S. Chang and U. Fano, Phys. Rev. A **6**, 173 (1972).
[15]R. Curik, F. A. Gianturco, and N. Sanna, J. Phys. B **33**, 2705 (2000).
[16]A. Jain and F. A. Gianturco, J. Phys. B **24**, 2387 (1991).
[17]E. Boronski and R. M. Nieminen, Phys. Rev. **34**, 3820 (1986).
[18]M. J. Frisch, G. W. Trucks, H. B. Schlegel *et al.*, Gaussian 09, Revision B.01, Gaussian, Inc., Wallingford, CT, 2003.
[19]W. L. G. Gent, J. Chem. Soc. **1957**, 58.
[20]D. G. Melnik, S. Gopalakrishnan, T. A. Miller, and F. C. De Lucia, J. Chem. Phys. **118**, 3589 (2003).
[21]B. Jansik, D. Jonsson, P. Salek, and H. Agren, J. Chem. Phys. **121**, 7595 (2004).
[22]N. Sanna, I. Baccarelli, and G. Morelli, Comput. Phys. Commun. **180**, 2544 (2009).
[23]N. Sanna, I. Baccarelli, and G. Morelli, Comput. Phys. Commun. **180**, 2550 (2009).
[24]N. Sanna and F. A. Gianturco, Comput. Phys. Commun. **114**, 142 (1998).
[25]A. Jain and D. G. Thompson, Comput. Phys. Commun. **32**, 367 (1984).
[26]L. Chiari, E. Anderson, W. Tattersall, J. R. Machacek, P. Palihawadana, C. Makochekanwa, J. P. Sullivan, G. Garcia, F. Blanco, R. P. McEachran, M. J. Brunger, and S. J. Buckman, J. Chem. Phys. **138**, 074301 (2013).
[27]A. G. Sanz, M. C. Fuss, F. Blanco, F. Sebastianelli, F. A. Gianturco, and G. Garcia, J. Chem. Phys. **137**, 124103 (2012).
[28]A. G. Sanz, F. Carrelli, F. Sebastianelli, F. A. Gianturco, and G. Garcia, New J. Phys. **15**, 013018 (2012).
[29]J. P. Sullivan, C. Makochekanwa, A. Jones, P. Caradonna, D. S. Slaughter, J. Machacek, R. P. McEachran, D. W. Mueller, and S. J. Buckman, J. Phys. B **44**, 035201 (2011).
[30]W. E. Kauppila, T. S. Stein, J. H. Smart, M. S. Dababneh, Y. K. Ho, J. P. Downing, and V. Pol, Phys. Rev. A **24**, 725 (1981).
[31]C. K. Kwan, W. E. Kauppila, R. A. Lukaszew, S. P. Parikh, T. S. Stein, Y. J. Wan, and M. S. Dababneh, Phys. Rev. A **44**, 1620 (1991).